Heliyon 9 (2023) e16567

Contents lists available at ScienceDirect

Heliyon

journal homepage: www.cell.com/heliyon

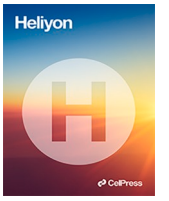

Research article

Ultra-tough artificial woods of polyphenol-derived biodegradable Co-polymer with Poly(butylene succinate)

Maninder Singh, Tatsuo Kaneko *

Energy and Environment Area, Graduate School of Advanced Science and Technology Japan Advanced Institute of Science and Technology, 1-1 Asahidai, Nomi, Ishikawa 923-1292, Japan

ARTICLE INFO

Keywords:
Bio-copolymers
Bioplastic
Ultra-tough
Polyphenols
poly(butylene succinate)
Biodegradable
Artificial wood

ABSTRACT

Large productions of plastics worldwide are greater concern to the environment because of their non degradability and thus, damaging the ecosystem. Recent advancements in biobased plastics are growing exponentially because of their promise of a sustainable environment. Biobased polycoumarates plastics have a wood-like appearance with liquid crystalline grains, light brown color, and cinnamon-like aroma, but have very low toughness. The polycoumarates were hybridized via main-chain transesterification with poly (butylene succinate) (PBS). PBS itself being a biobased material has added more value to the final product due to biodegradability. The mechanical flexibility and toughness of the bio-based copolymers were controlled by varying the PBS content. As a result, well-processable and in-soil degradable artificial woods with a high strain energy density of approximately 76 MJ/m^3 were developed while maintaining the wood-like appearance.

1. Introduction

Wood has attracted enormous attention because of its biodegradability, light weight, high mechanical toughness, and nontoxic chemical composition [1–4]. However, the requirement for material reproducibility has widened artificial forest areas with low diversity of tree species, damaging the environment. Thus, bottom-up strategies have been employed to develop wood-like materials also known as "artificially engineered wood" [5–9]. The wood drawbacks such as instability and limited processability have activated the field [10,11]. In order to produce hierarchical structures modeled after balsa wood, Brett et al. reported epoxy-based inks that enable 3D printing of cellular composites with the controlled alignment of multiscale, high-aspect-ratio fiber reinforcement. The Young's moduli of commercially accessible 3D-printed polymers, which are made from thermoplastics and photocurable resins created specifically for industrial 3D printing processes, are greater than those materials [12]. Pan et al. have developed xylem-like monoliths (XMs) with honeycomb-like penetrating microchannels using unidirectional freeze-drying approach [13]. However, the use of toxic chemicals in the production of artificial wood and its non-degradability in the environment are still problematic and thus invite alternative designs that utilize biobased bottom-up strategies to develop the artificially engineered wood [14–16]. We previously developed environmentally-degradable aromatic biobased polyesters using phenolic bio-monomers such as *p*-coumaric acid (4-hydroxycinnamic acid; 4HCA), *m*-coumaric acid (3-hydroxycinnamic acid), 3-methoxy-4-hydroxycinnamic acid (ferulic acid), and caffeic acid (3,4-dihydroxycinnamic acid; DHCA), showing better thermal and mechanical performances than conventional biobased

* Corresponding author.
E-mail address: kaneko@jaist.ac.jp (T. Kaneko).

https://doi.org/10.1016/j.heliyon.2023.e16567
Received 13 December 2022; Received in revised form 17 May 2023; Accepted 19 May 2023
Available online 22 May 2023

polyesters [17–19]. In addition, the co-polyester resin had light-brown color and thermotropic liquid crystalline to show banded texture on the surface and then the appearance was more woody than real wood [20–22]. However, low mechanic flexibility and toughness prevented commercial application of these materials in polymer electronics with high deformation ability.

At the same time, there are flexible polyesters, such as polybutylene succinate (PBS), which has an aliphatic chain derived from 1,4-butanediol and succinic acid [23–25]. PBS shows good biodegradability in the environment, and some of its derivatives have been registered as biodegradable polymers in marine environments [24,26]. PBS finds its place in various flexible polymer applications, such as foamed sheets, bottles, films, and many other disposable products [27,28]. Zhang combined PBS with poly (lactic acid) (PLA) to enhance the mechanical properties. Obtained polymer copolymerss showed greater elongation at break and impact strength than short block chains [29]. Platnieks et al. utilized PBS with cellulose to prepare wood-like materials to produce stabilized wood-like materials [30].

This study presents a novel approach to fabricating flexible and durable bioplastics. By incorporating PBS into the aromatic matrix of poly (4HCA-*co*-DHCA)s using a one-step fabrication strategy, we were able to create a final product that resembles wood in appearance. This innovation holds significant potential as a sustainable alternative to traditional wood materials and could be utilized across a wide range of industries. We believe that our development of artificially engineered woods will pave the way for exciting advancements in material science and contribute to a more sustainable future.

2. Experimental section

2.1. Materials and methods

4HCA (Tateyama Kasei co. ltd) and DHCA (Tateyama Kasei co. ltd) obtained as monomers were used as received without further purification. PBS (copolymer of 1-butanol and Succinic acid, Grade: FD92) was provided from Mitsubishi Chemical Co. Ltd., Japan and were used as received without further purification. Acetic anhydride (Wako Pure Chemical Industries, Ltd., Japan) and sodium acetate (Wako Pure Chemical Industries, Ltd., Japan) used for polymerization were used as received. Polylactic acid (PLA) was used as a composting reference (TCI, Japan). Acetone (Wako Pure Chemical Industries, Ltd., Japan) used as a washing solvent was used as received. Dimethylformamide (DMF; Wako Pure Chemical Industries, Ltd., Japan) and DMF-d_7 (Wako Pure Chemical Industries, Ltd., Japan) were used as received.

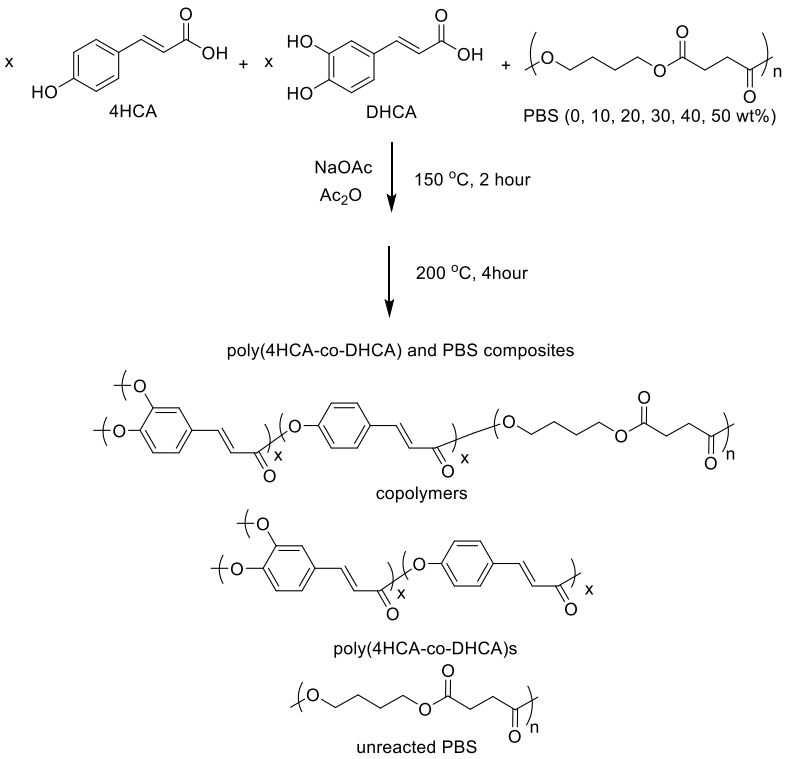

Scheme 1. Synthetic process of copolymers for poly (4HCA-*co*-DHCA) and PBS. 4HCA and DHCA was acetylated and polymerized by acidolysis reaction in the presence of PBS. Resulting copolymers can be comprising poly (4HCA-*co*-DHCA)s, PBS, and their copolymers.

2.2. Syntheses of PBS copolymers

DHCA (50 mmol), 4HCA (50 mmol), PBS (0, 10, 20, 25, 30, 40 and 50 wt% to total of 4HCA and DHCA) were taken together in a three-neck flask fitted with nitrogen inlet, mechanical stirrer, and nitrogen outlet. Acetic anhydride (40 ml) and sodium acetate (1 wt %) was added into the flask as acetylation reagent and acidolysis catalyst, respectively. Nitrogen was gassed into the flask for 1 h at room temperature with constant stirring. The reaction mixture was heated to 150 °C and maintained for 2 h under agitation. The temperature was further raised to 220 °C and reaction mixture was kept for another 4 h in vacuo as shown in Scheme 1. The reaction solution increased its viscosity gradually and was finally solidified not to allow further stirring. After the reaction was finished by cooling to room temperature, the materials were milled into a powder and purified by washing with acetone two or three times (yields: 80−90 wt%). Samples with PBS compositions of 0, 10, 20, 25, 30, 40, 50, and 100 (neat PBS) weight % are referred to as PB 0, PB 1, PB 2, PB 2.5, PB 3, PB 4, PB 5, and PBS, respectively.

2.3. Enzymatic degradation of PBS copolymers

Enzymatic degradation of the polyester copolymers (PB 4) was investigated using lipase enzyme. The samples were formulated into rectangular strip with dimension of 0.5 cm length, 0.5 cm width, and 1 mm thickness using manual hydraulic press with pressure of 10 MPa. Sample was placed in an individual flask and incubated at 37 °C in phosphate buffer solution (pH = 8.4) and 0.6 mg/ml lipase. Sample were taken out, gently wiped with filter paper, dried at room temperature in a desiccator for 24 h and subjected to GPC analysis at 3rd week and 5th week. Control experiments were carried out for same polyester copolymers sample by incubation in buffer solution in the absence of the enzyme and GPC analysis was done to observe the change in the molecular weight. The enzyme treated co-polymers were taken out of flask dried and quantitative analysis was done using ^{1}H NMR in deuterated d_2-CD_2Cl_2.

2.4. In-soil degradation

In-soil degradation of the polyester copolymers (PB 4) were investigated by burying the copolymer samples under the soil (10 cm beneath). A rectangular piece of PB 4 copolymer material had been buried in soil for 10 months (JAIST, Ishikawa, Japan) along with the PLA as a control sample.

Samples were taken out after every 2 months, gently wiped with filter paper, and the final weight was noted. The weight loss of the copolymers sample was assessed by following formula for each sample.

$$D = (W_0 - W_t)/W_0 \times 100$$

Where W_0 is the initial weight of each sample and W_t is the weight of the sample at time t. Initial weight of both PB 4 copolymers and PLA were taken to calculate the weight loss during 10 months of the testing period.

2.5. Bio-copolymers characterizations

Chemical shifts for the protons were recorded for all the copolymers samples using ^{1}H nuclear magnetic resonance (^{1}H NMR) spectroscopy (Bruker 400 MHz, Japan). All the copolymers and neat PBS for ^{1}H NMR were prepared using dichloromethane (d_2, CD_2Cl_2). Thermogravimetric analysis (TGA) was carried out using TA instrument (TGA, Hitachi TA7000, Japan). All the copolymers and neat PBS were placed into a platinum pan and heated to 800 °C at a temperature ramp rate of 10 °C/min under a nitrogen environment. The tests were carried out in duplicates.

The copolymers were subjected to XRD analysis using X-ray diffraction (XRD; Rigaku Smart Lab with Cu K_α) to check the crystallinity in the samples. The phase transition of poly (4HCA-*co*-DHCA)s was observed using a crossed-polarizing microscope (Olympus BX51) equipped with a digital camera. The samples were sandwiched between two glass plates and were heated at a rate of 10 °C/min (resolution: ±0.1 K) by a METTLER TOLEDO FP82HT Hot Stage (Greifensee, Switzerland).

Differential scanning calorimetry (DSC) was performed using a TA instruments (DSC, X-DSC7000T, Hitachi, Japan). For each copolymers sample, 3–5 mg of sample was sealed in an aluminium pan, which was heated from room temperature to 150 °C at a rate of 10 °C/min and held at that temperature for 10 min, then cooled to −30 °C with liquid nitrogen at a rate of 5 °C/min and held for 2 min. Second and third scan were done using the same temperature profile. The nitrogen flow was kept at 200 ml/min throughout the test. The samples were dried overnight under vacuum prior to testing. Samples were tested in duplicate to authenticate the final values. The second heating cycle and first cooling cycle were used for analysis and tests were done in duplicates. Glass transition temperature (T_g), was calculated using these cycles.

Fourier transform infrared (FT-IR) spectra were recorded on a PerkinElmer spectrometer using a diamond-attenuated total reflection (ATR) accessory between 4000 and 400 cm^{-1} with 4 consecutive scans at a resolution of 2 cm^{-1} under an air atmosphere to analyse the functional groups.

The molecular weight of the copolymers were determined by gel permeation chromatography (GPC) using a Shodex GPC-101 was calibrated with polystyrene standards (eluant: dimethylformamide)\equipped with a reflective index detector (RI-2031 Plus, JASCO, Tokyo, Japan) and an ultraviolet detector (UV-2075 Plus, JASCO, Tokyo, Japan) was used to determine the number-average molecular weight (M_n), weight-average molecular weight (M_w), and the molecular weight distribution (PDI). Copolymer samples (10 mg) for molecular weight analysis were dissolved in DMF (1 ml). After solubilisation, the solution was filtered to remove the remaining

residue.

To understand the surface morphology of the prepared copolymers, scanning electron microscopy (SEM) was performed with a JEOL (JEOL, Netherlands) equipped with back scattering electron at 10 kV acceleration voltage. The samples used for the SEM images were fractured with a pendulum hammer to provide a cross section for imaging. The PBS copolymers were moulded into the rectangular test pieces (5 cm L × 5 cm W × 0.5 cm T) by hot press (10 MPa, 70 °C for 10 min). The three-point bending was tested using a compress testing machine (INSTRON, 3365-L5). The samples were set over two fixtures 30 mm apart, and the centre of each sample was pressed from the opposite direction. All tests were carried out at 25 °C using a fixed nominal displacement rate of 1 mm/min. The data of at least three samples were averaged.

3. Results and discussion

3.1. Preparation of copolymers

Copolymerization of 4HCA and DHCA (equimolar feed composition) was performed in the presence of acetic anhydride and PBS to prepare copolymers of poly (4HCA-*co*-DHCA)s with PBS. One sample without PBS (PB 0) and six samples with different weight% of the PBS (PB 1, PB 2, PB 2.5, PB 3, PB 4, PB 5) were prepared, as shown in Scheme 1. The phenolic groups of 4HCA and DHCA should react with acetic anhydride at 150 °C to produce acetylated monomers, although only a trace amount of PBS hydroxyl ends could also be acetylated to avoid affecting the reaction system. Acetylated monomers were polymerized in the presence of NaOAc as an acidolysis catalyst at 200 °C in vacuo, where the carboxylate group of the monomers attacked aliphatic esters to eliminate aliphatic carboxylates. The monomer carboxyls attacked PBS esters in the acidolysis reaction mechanism to produce two main types of block copolymers composed of two blocks: PBS and poly (4HCA-*co*-DHCA)s, diblock, and triblock copolymers, as shown in Scheme 1. Although multiblock copolymers might also be formed by transesterification of the acetyl ester monomer with PBS esters, the probability is negligibly low. The excess acetic anhydride and eliminated acetic acid were evaporated under vacuum, and the viscosity of the reaction mixture gradually increased until solidification, which would not allow further stirring. Aromatic polyesters Poly (4HCA-*co*-DHCA)s were intrinsically immiscible with aliphatic polyester PBS, but these polyesters did not appear phase-separated during

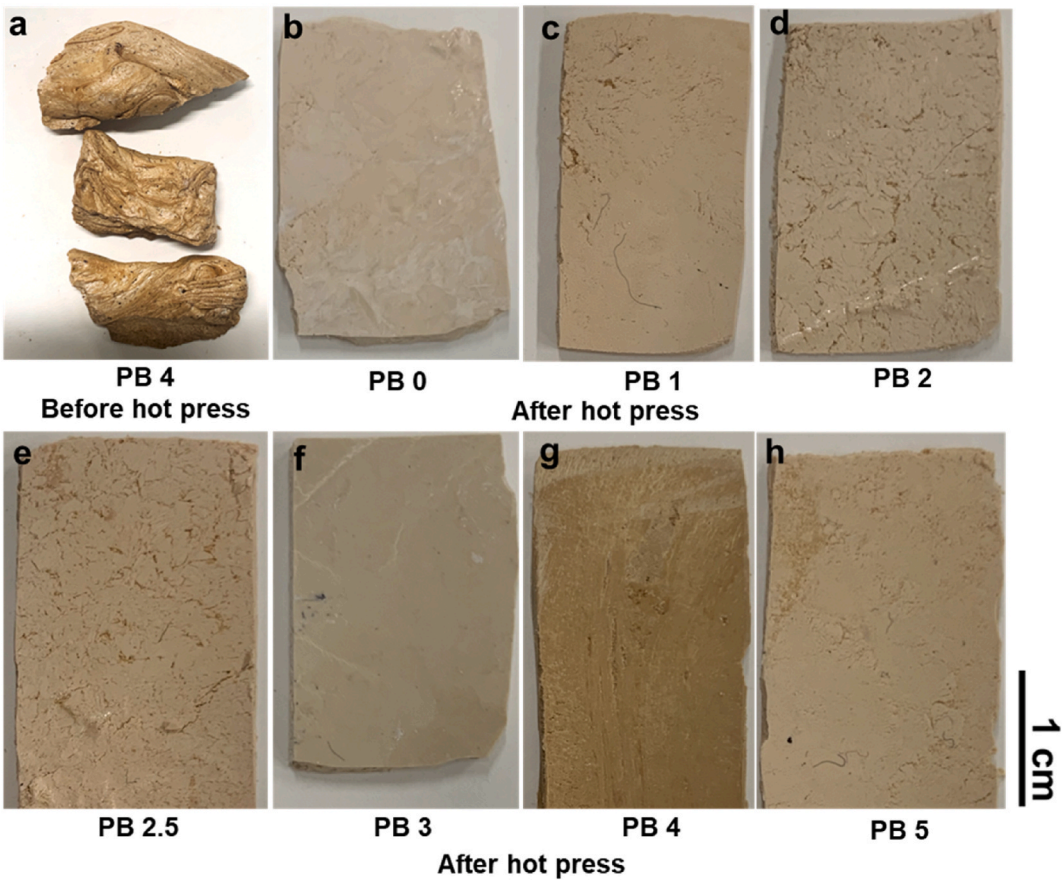

Fig. 1. Actual picture of the copolymers before and after hot press depicting the woody appearance of the copolymers. Copolymer sample a) PB 4 before hot press and copolymer samples (b–h) PB 0, PB 1, PB 2, PB 2.5, PB 3, PB 4, PB 5 after hot pressing.

polymerization, presumably because of the role of block copolymers acting as compatibilizers. As a result, a homogeneous mesoscopic copolymers was formed, as confirmed by the SEM image (Fig. 2) of the copolymers. In the reported work, a polymer blend compatibilizer introduces an interfacial active polymer that improves miscibility with the polymer blend component. The blocks can be chemically or structurally identical to a blend component, or they can include functionalities that allow chemical interactions with particular blend components, all of which promote miscibility of one block into each polymer mix component [29]. The final product was mechanically milled into powder, and the remaining acetic acid derivatives were washed with acetone two or three times before further characterization. The resulting dried powders were then cast into rectangular shapes using a hot press machine. Actual pictures of the copolymers before and after hot pressing are shown in Fig. 1, which confirms the wood-like appearance of the copolymers.

3.2. Structural analysis of copolymers

The successful syntheses of PBS and seven copolymers: PB 0, PB 1, PB 2, PB 2.5, PB 3, PB 4, and PB 5 were confirmed using ^{1}H NMR spectroscopy, as shown in Fig. 3. ^{1}H NMR for poly (4HCA-*co*-DHCA) (Fig. S1a) showed proton signals at ranges of $\delta = 2.20$–2.43 ppm (acetyl protons), $\delta = 6.60$–6.82 ppm (α-CH), $\delta = 7.13$–7.82 ppm (aromatic protons), and $\delta = 7.82$–8.18 ppm (β-CH). This assignment confirmed the synthesis of poly (4HCA-*co*-DHCA). The detailed assignment of the branching of PBS with DHCA and 4HCA units is shown in Figs. S1(b–d), and the ^{1}H NMR spectra of PB 1, PB 2, PB 3, PB 4, PB 5, and PBS (copolymers of poly (4HCA-*co*-DHCA) with different wt.% of PBS). The molar amount of acetyl end groups, C_{acetyl}, should be equal to $C_{\text{DHCA}} + 1$, where C_{DHCA} is the moles of DHCA, in this hyperbranching system from the AB_2 monomer. If the polymerization degree is sufficiently high, C_{acetyl} is almost equal to C_{DHCA}. Representative ^{1}H NMR and calculations of the molar fraction of PBS incorporated into the copolymers material for sample PB 5 are shown in Fig. S2. The molar fractions of PBS ($W_{\text{PBS}}^{\text{NMR}}$) incorporated into the copolymers material of HCA and DHCA were calculated from the integral signal intensities (I) in the ^{1}H NMR of the respective copolymers materials using the following formula, and the actual values are summarized in Table 1.

$$W_{\text{PBS}} = \frac{I_{\text{PBS}}}{I_{\text{HCA+DHCA}} + I_{\text{PBS}}} \times 100$$

The calculated mole fractions of PBS are slightly lower than the theoretical values, which is possibly caused by the formation of oligomeric degrades that were removed by reprecipitation.

The functional groups of the resulting copolymers were further analyzed using FTIR, as shown in Fig. 4. Aromatic and aliphatic ester linkages (C═O) were detected in the wavenumber range of 1700–1765 cm^{-1} for all the copolymers. Moreover, C═C vibrations for the aromatic and vinylene groups were observed in the wavenumber range of 1530–1600 cm^{-1} for all the copolymers except the aliphatic PBS. Aromatic/aliphatic esters were not detected.

3.3. Crystallinity of copolymers

The X-ray diffraction patterns of PB 0, PB 1, PB 2, PB 2.5, PB 3, PB 4, PB 5, and PBS are shown in Fig. 5a. PB 0 shows a broad peak around a diffraction angle $2\theta = 22.0^\circ$, indicating an amorphous phase. At the same time, PBS showed two intense diffraction peaks at 22.9° and 19.9°, indicating crystalline polymers (Fig. 5b). For the copolymers, it was clearly observed that the crystalline peaks became sharper and more intense as the PBS content increased. The relative crystallinity was estimated quantitatively from XRD measurements using the approach used by Nara and Komiya et al. [31] The crystallization degrees of the copolymers increased from 5 to 30% with the PBS content and were almost linear (Fig. 6).

This tendency indicates the homogeneity of all copolymers irrespective of the composition. The liquid crystalline behavior was also studied for all the copolymers samples. It was found that the copolymers sample without PBS, that is, PB 0, showed liquid crystallinity, which decreased with an increase in the PBS wt.% in the polyester copolymers, as shown in Figure S4. In Figure S4, Cross-polarised images of different bio copolymers were observed at 220 °C using crossed-polarizing microscopy. Cross-polarised microscopy revealed that the copolymer samples melted at particular temperatures to demonstrate a thermotropic liquid crystalline phase. The schlieren

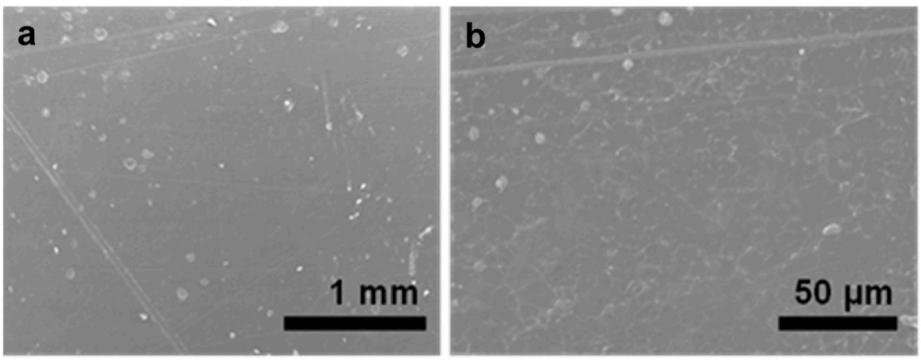

Fig. 2. SEM image of copolymers PB 4 showing homogeneity. a) and b) are the SEM mages of the copolymer PB 4 showing the homogeneity.

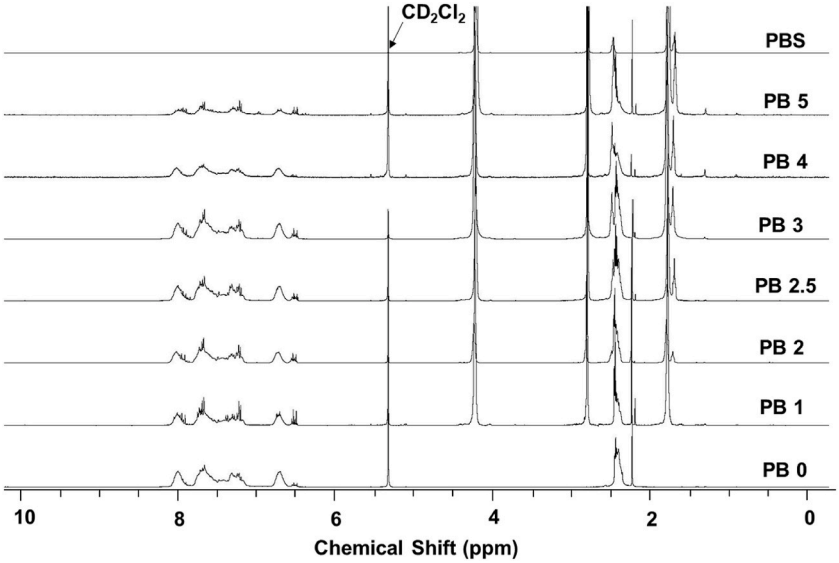

Fig. 3. [1]H NMR spectra of poly (4HCA-*co*-DHCA) with PBS.

Table 1
Molar fractions of PBS in copolymers materials with HCA and DHCA.

Samples	W_{HCA} (mol %)	W_{DHCA} (mol %)	W_{PBS} (mol %)	W_{PBS}[a] (mol %)
PB 0	50.0	50.0	0	0
PB 1	45.0	45.0	10.0	9.0
PB 2	40.0	40.0	20.0	11.4
PB 2.5	37.5	37.5	25.0	16.3
PB 3	35.0	35.0	30.0	26.5
PB 4	30.0	30.0	40.0	37.3
PB 5	25.0	25.0	50.0	46.1
PBS	0	0	100.0	100.0

[a] WPBS is calculated using NMR using the integral strength ratio of PBS and poly (HCA-*co*-DHCA).

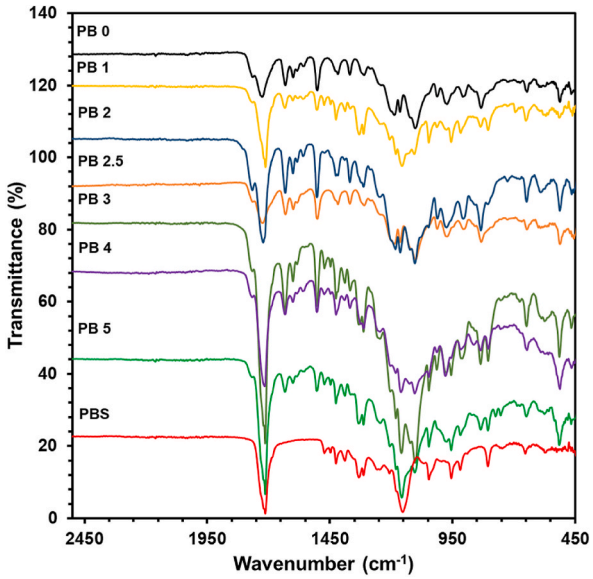

Fig. 4. FTIR spectrograms for copolymers of poly (4HCA-*co*-DHCA) with PBS.

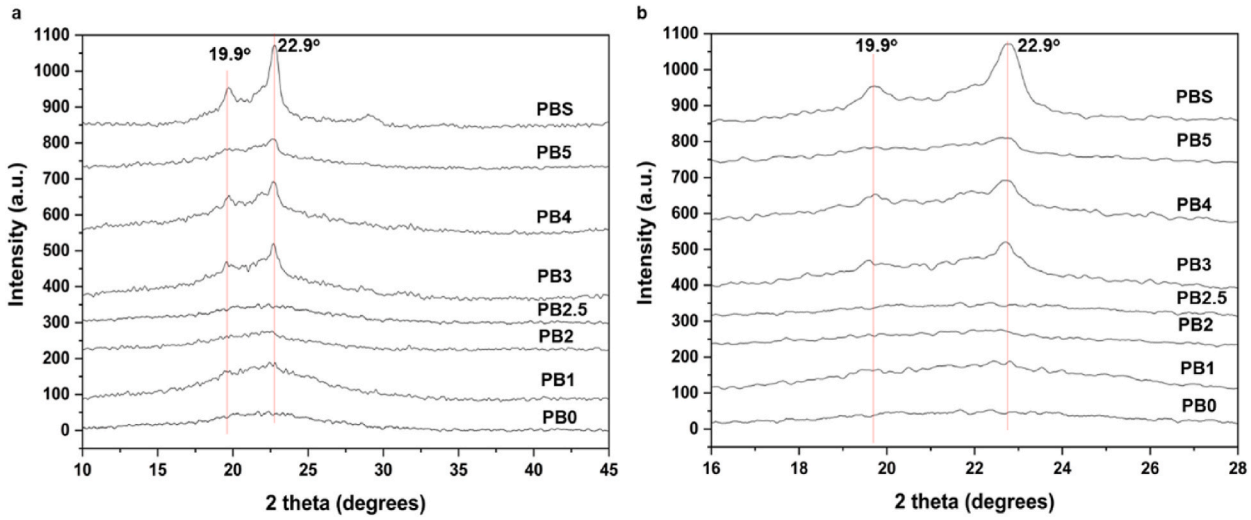

Fig. 5. X-Ray diffractograms (a) for all the copolymers samples, and (b) enlarged view for all the samples in the 2θ: 16–28°.

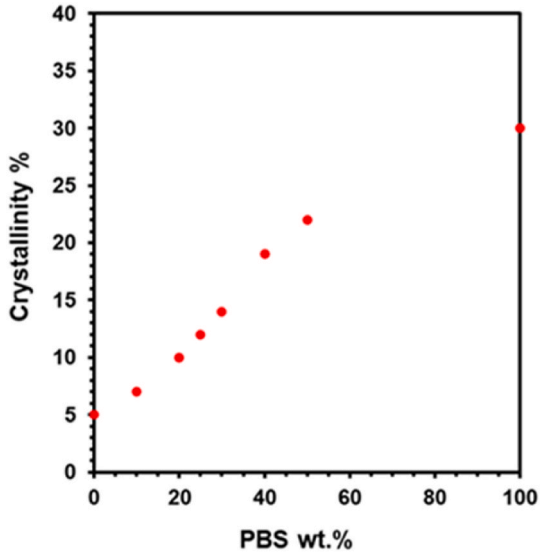

Fig. 6. Plot representing crystallinity with respect to change in the weight % of PBS.

texture indicative of a nematic state was observed for samples PB0, PB1, PB2, PB3, PB4 but PBS showed spherulitic morphology.

3.4. Thermal properties

The thermal properties of poly (4HCA-*co*-DHCA), PBS, and their copolymers were analyzed using TGA and DSC. Fig. 7 clearly shows that PBS has a higher thermal degradation temperature than poly (4HCA-*co*-DHCA) because of the relatively low stability of the vinylene group in 4HCA and DHCA [32–34].However, the char yield of poly (4HCA-*co*-DHCA) was much higher than that of PBS owing to its aromaticity. For the copolymers, the thermal degradation temperatures, T_{d1}, T_{d5}, and T_{d10}, increased with the weight percentage of PBS in the copolymers. The T_g values of the copolymers were lower than that of poly (4HCA-*co*-DHCA) and higher than that of PBS, as listed in Table 2 and DSC curves shown in Figure S3. Figure S3 describes the second heating cycle of DSC run. It can be clearly seen that on increasing the PBS wt. % in copolymer matrix, the T_g value (first shoulder downwards) is shifting to lower temperatures. It means that the material becomes softer and more flexible. Thus, a decrease in T_g can lead to increased flexibility, and elongation at break. The T_g of the copolymers ranged from 66 to 124 °C, which is higher than those of previously reported biodegradable polymers [35].

The copolymers were not soluble in most of the solvents used here as shown in Table S1. Pentaflurophenol and TFA/DCM (1/5 v/v %) were identified as the good solvents for all the copolymers with different PBS composition. Solubility data of all the monomers, and

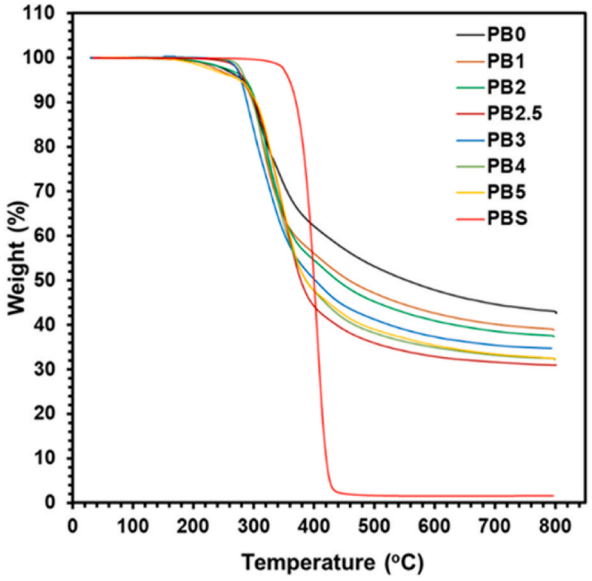

Fig. 7. Thermal degradation properties of poly (4HCA-*co*-DHCA-*co*-PBS).

Table 2
Thermal degradation and mechanical properties of poly (4HCA-*co*-DHCA-*co*-PBS).

Samples	T_g[b] (°C)	T_{d0}[b] (°C)	T_{d5}[b] (°C)	T_{d10}[b] (°C)	X_c[c] (%)	$M_n \times 10^5$	$M_w \times 10^5$	PDI	σ[a] (MPa)	E[a] (GPa)	ε[a]	Φ (MJ/m^3)	Ref.
PB 0	124	164	254	270	5	3.1	6.7	2.1	50 ± 0.3	116 ± 1.2	0.6	2 ± 0.6	*
PB 1	78	186	221	270	7	3.2	6.6	2.0	19 ± 0.7	10 ± 0.3	0.5	2 ± 0.6	*
PB 2	66	201	234	270	9	3.4	6.4	1.9	22 ± 0.5	12 ± 0.3	0.3	7 ± 1.0	*
PB 2.5	66	204	240	272	12	4.1	6.4	1.9	41 ± 0.9	28 ± 0.8	0.2	18 ± 3.0	*
PB 3	66	238	279	300	17	4.0	7.0	1.7	158 ± 3.3	90 ± 1.8	1.5	69 ± 11.5	*
PB 4	67	238	285	300	20	4.5	6.9	1.5	125 ± 2.1	81 ± 0.9	1.3	76 ± 16.0	*
PB 5	67	240	290	310	24	4.4	7.0	1.6	199 ± 1.1	111 ± 1.4	–	–	*
PBS	−47	317	356	368	30	9.1	2.3	3.9	–	–	–	–	*
PHB	5	–	–	–	–	–	–	–	35.0	4.0	–	–	[36]
PLA	52.5	–	–	–	1.4	–	–	–	42.0	2.0	–	–	[37]
PC	157	–	–	–	–	–	–	–	55	2.0	–	–	[38]
PCL	−54	–	–	–	43.7	–	–	–	24	0.3	–	–	[39]
Silicon rubber	−123	–	–	441	–	–	–	–	8	–	–	200	[40]
Raw bamboo	–	–	–	–	–	–	–	–	135	9	–	–	[41]
Sitka spruce	–	–	–	–	–	–	–	–	67	8	–	–	[42]
Douglas-fir LVL	–	–	–	–	–	–	–	–	68	13	–	–	[43, 44]
Bleached bamboo	–	–	–	–	–	–	–	–	77	10.3	–	–	[41]

*This work.
[a] The mechanical properties were measured by a stress–strain bending test. 'σ' 'E' 'ε' and 'Φ' refer to flexural strength, flexural modulus, maximal strain and strain energy density respectively.
[b] T_g, and T_{d10} values are measured using DSC and TGA, respectively.
[c] X_c (%) values are measured using XRD.

copolymers samples in various solvents were summarized in Table S1.

3.5. Mechanical properties

Three-point bending analysis was performed on poly (4HCA-*co*-DHCA), PBS, and their copolymers. PB 5 and PBS test specimens were too soft to show the relevant data in the bending mode. Sample PB 0 is a very rigid material, as can be inferred from the mechanical properties (Table 2) but lacks flexibility. To induce flexibility, PBS was combined as a flexibility inducer at different wt.% with

4HCA and DHCA.

The flexural strength (σ), modulus (E), and maximal strain (ε) of the polyester copolymers materials are shown in Fig. 8a. As shown in Fig. 8b, the mechanical strength of the resulting copolymers materials increased with the PBS wt.%, which in turn resulted in high flexural modulus (Fig. 8c) of these copolymers materials. As a result, it was found that the flexibility and toughness of the copolymers were controlled by PBS composition (Fig. 8d). Here, we can emphasize that an appropriate composition of PBS drastically increased the toughness of the copolymers resins to 76 MJ/m^3, approaching that of the silicone rubber. Such a high level of toughness was attributed to the appropriate structural balance of rigid polyphenols and flexible PBS, possibly compatibilized by the block copolymers. The flexural strength and modulus increased as the PBS unit ratio increased, demonstrating that the crystalline phase formed from the PBS unit increases the hardness of the PB 5 copolymer. This finding suggests that the poly (4HCA-*co*-DHCA) unit disrupts the crystallinity of the PBS unit and provides great flexibility to PBS, a hard plastic [26].Strain energy density data was calculated based on the mechanical behavior of all the copolymers samples, as shown in Fig. 8 and Table 2.

4. Degradation of copolymers

4.1. Enzymatic degradation

The PB 4 copolymers was tested for enzymatic degradation. A small amount (150 mg) of PB 4 (Mw: 24,300–26400 g mol^{-1}) with 1 wt% of lipase B (5 ml) in a pH 8.4 buffer was taken to study the polyester degradation. Control experiments were performed without lipase B. The samples were shaken in an incubator for 5 weeks at 37 °C. The Mw of the copolymers polyesters over time was monitored using GPC. Mw decreased from 24,300 to 26400 g mol^{-1} to 14,600–16500 g mol^{-1} in the presence of lipase B over 5 weeks. The molecular weight loss of the copolymers sample over the course of 5 weeks is shown using the GPC curves in Fig. 9. A significant shift of the peaks to the right shows that the molecular weight decreased over the course of 5 weeks of enzymatic degradation.

The results showed that 60% of the weight loss occurred within 5 weeks. Sample degradation was also monitored using ^{1}H NMR of the degraded sample in the presence of the enzyme and compared with that of the original sample shown in Figure S5 (Supporting Information). The ^{1}H NMR signals of the supernatant of the sample immersed in lipase B solution for 5 weeks were much sharper than those of the original samples, indicating that the dissolution of the samples reduced the molecular weight. Degradation of the PB 4 copolymers sample was also investigated in the absence of the enzyme. The sample showed no significant loss in molecular weight, as confirmed by GPC (Figure S7). The enzyme acts as a hydrolysis catalyst [45–47] for the aliphatic ester bonds formed by polycondensation, reverting the polymer into raw materials: hydroxy cinnamic acid and PBS. The completely aromatic polyester sample PB 0 was also tested for lipase-catalyzed degradation using ^{1}H NMR, as shown in Fig. S6, indicating no change in the peaks. Even ^{1}H NMR peaks were not observed in the supernatant. This confirmed that lipase had no degrading effect on the aromatic polyesters.

4.2. In-soil degradation

The PB 4 copolymer was also tested for in-soil degradation. A rectangular piece of PB 4 copolymers material buried in the soil for 10 months showed deformation (Fig. 10b). The buried copolymers material showed 5–10% weight loss, whereas the PLA buried with the copolymers material did not show deformation or weight loss. Moreover, SEM micrographs of the deformed poly (4HCA-*co*-DHCA-*co*-PBS) samples showed that the surface of the copolymers material was deformed, in contrast to the smooth surface of the non-degraded compact copolymers material (Fig. 10a), whereas the buried PLA had a flat surface and did not show any deformation, as confirmed by the SEM image of the PLA before and after burying into the soil (Figure S8). These observations show that in-soil degradation of the compact copolymers material occurred via microbial action. The weight loss profiles of both PB 4 and PLA over the course of several months of burying in soil are shown in Figure S9, which clearly shows that the PB4 polyester material degrades with time, presumably because of the interaction with the microorganisms in the soil [48–50]. Up to 10% weight loss was observed during in-soil degradation for 10 months, whereas no change in weight was observed for PLA, which was used as the control sample.

5. Limitations and future prospects

While the incorporation of polybutylene succinate (PBS) as a flexibility inducer has resulted in successful fabrication of flexible bioplastics, certain limitations have been encountered. One such limitation is the inability to incorporate more than 50 wt% of PBS into the polymer matrix. At higher concentrations, the polymer becomes extremely soft and sticky, making it difficult to process into different forms such as blocks or films.

One potential solution is to use other biopolymers that can provide similar flexibility but with higher tolerance to higher concentrations. Such biopolymers would need to be easily processable at high concentrations while maintaining their physical properties. Researchers are exploring different biopolymer candidates and evaluating their suitability as a PBS substitute.

The search for a suitable PBS substitute is crucial as the demand for bioplastics continues to grow. Bioplastics offer several environmental benefits over traditional petroleum-based plastics, including reduced greenhouse gas emissions and reduced dependence on fossil fuels. However, their potential is limited by their processability, which can be improved by identifying and using alternative biopolymers that can overcome the limitations of PBS.

In summary, while PBS has been successful in providing flexibility to bioplastics, its limitations in terms of processability at higher concentrations are a concern. Identifying and using alternative biopolymers that can provide similar flexibility while maintaining their physical properties and processability is an important area of research for the development of bioplastics with improved performance

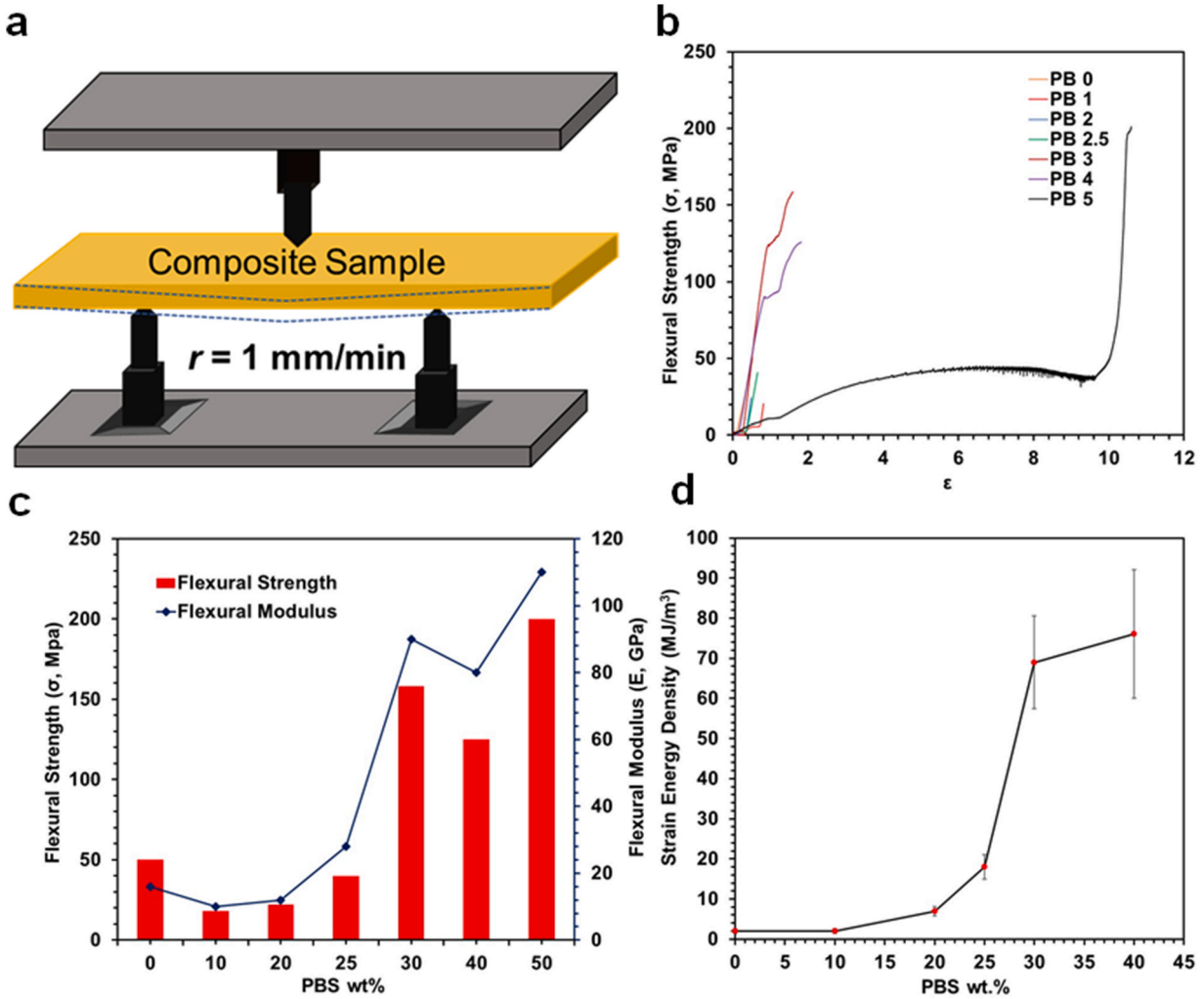

Fig. 8. (a) Schematic of the rectangular samples used for the 3-point bending analysis, (b) Stress-Strain curve for the copolymers. (c) Flexural strength (σ) and flexural modulus (E) of the copolymers with respect to PBS compositions. (d) Strain energy density (Φ) of the copolymers with respect to PBS composition.

and versatility.

6. Conclusions

Flexible and tough bio-based copolymers were prepared via polycondensation of biobased monomers 4HCA and DHCA in the presence of a biodegradable polyester, PBS. Spectroscopy results confirmed the formation of the aromatic copolymer poly (4HCA-*co*-DHCA) and copolymers with the PBS block via the acidolysis of 4HCA and DHCA with PBS esters. These copolymers may act as compatibilizers of poly (4HCA-*co*-DHCA) and PBS to produce homogeneous copolymers. An increase in the PBS content enhanced the thermal degradation temperature and mechanical toughness. In particular, the copolymers of poly (4HCA-*co*-DHCA) with 40 wt% PBS (PB4) had a high strain energy density of 76 MJ/m^3 and exhibited enzymatic and in-soil degradation. Over the course of 5 weeks, *M*w for sample PB4 decreased from 24,300 to 26400 g mol^{-1} to 14,600–16500 g mol^{-1}. After in-soil deterioration for 10 months, up to 10% weight loss had been observed for sample PB4, while for PLA, the control sample, there was no weight change. This durable biodegradable resin has a brown wood-like appearance and can be applied as an artificial wood material in a future sustainable society.

First author

Maninder Singh – Graduate School of Advanced Science and Technology, Japan Advanced Institute of Science and Technology, 1-1 Asahidai, Nomi, Ishikawa, 923 1292, Japan. ORCID: orcid. org/0000-0002-9759-2131, Phone: +81-761-51-1633 E-mail: maninder@jaist.ac.jp.

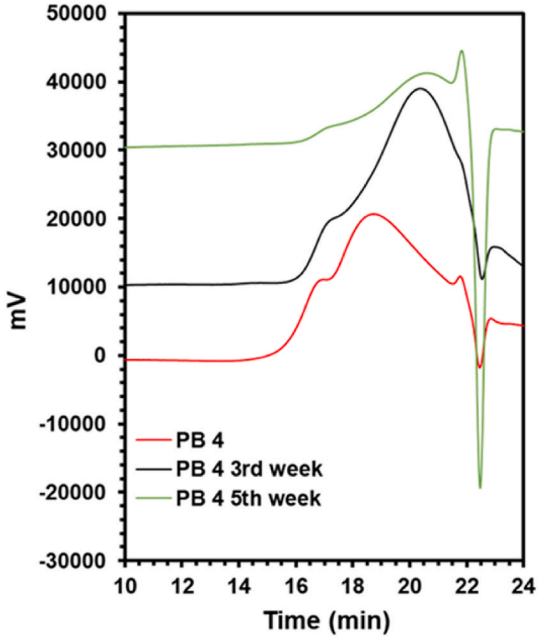

Fig. 9. GPC chromatogram of the PB 4 copolymer in the presence of lipase over span of 5 weeks.

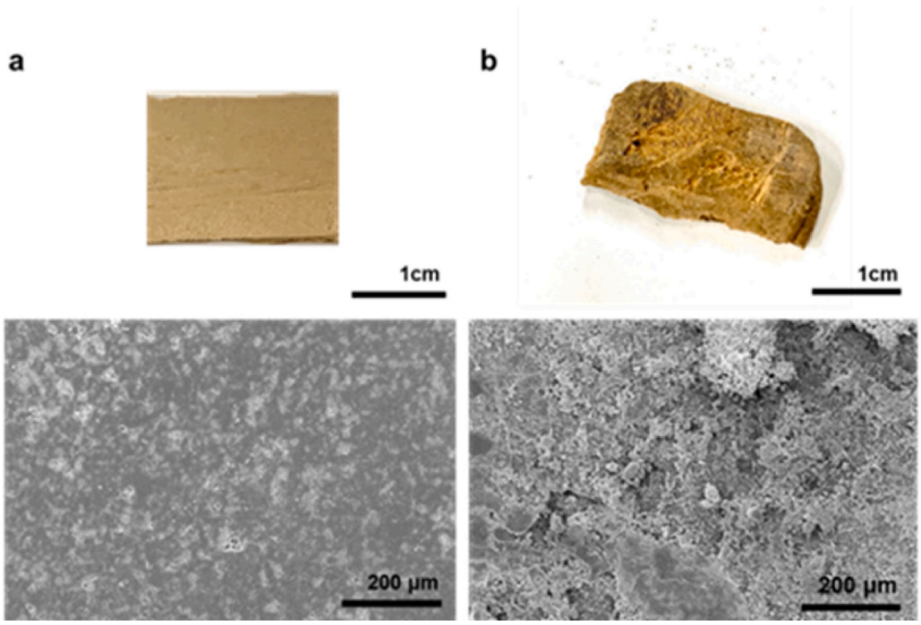

Fig. 10. Photos of the PB 4 copolymer sample before and after burying in the soil for 10 months. (a) Macroscopic digital image and SEM image of the sample surface before burying in the soil, (b) Macroscopic digital image and SEM image of the sample surface buried in the soil (JAIST, Ishikawa, Japan) showing surface degradation.

Author contribution statement

Maninder Singh: Conceived and designed the experiments; Performed the experiments; Analyzed and interpreted the data; Contributed reagents, materials, analysis tools or data; Wrote the paper.

Tatsuo Kaneko: Contributed reagents, materials, analysis tools or data.

Data availability statement

Data will be made available on request.

Funding sources

The funding is provided by Moonshot project, JPNP18016.

Declaration of competing interest

The authors declare that they have no known competing financial interests or personal relationships that could have appeared to influence the work reported in this paper

Acknowledgment

This paper is based on results obtained from a Moonshot project, JPNP18016, commissioned by the New Energy and Industrial Technology Development Organization (NEDO), Japan. Authors also would like to thank Mitsubishi Chemicals Pvt. Ltd., Japan for providing PBS.

Appendix A. Supplementary data

Supplementary data to this article can be found online at https://doi.org/10.1016/j.heliyon.2023.e16567.

Supplementary Information

Supplementary information provides ^{1}H NMR data for all the non-PBS and PBS samples with different weight percent, solubility data, DSC curves for PB 1, PB 2, PB 2.5, PB 3, PB 4, PB 5 and PBS, cross-polarised images of all the copolymers, ^{1}H NMR data confirming enzymatic degradation, GPC chromatogram of PB 4 copolymers in absence of lipase over span of 5 weeks, SEM images of the control PLA before, and after burying into the soil (JAIST, Ishikawa, Japan) for 10 months, weight loss profile of the copolymers samples *i.e.*, PB 4 and PLA during several months of burying into the soil.

Abbreviations

XMs	xylem-like monoliths
4HCA	4-hydroxycinnamic acid
DHCA	3,4-dihydroxy cinnamic acid
PBS	poly(butylene succinate)
PLA	poly lactic acid

References

[1] V.A. Barbash, O. V Yashchenko, V.O. Opolsky, Effect of hydrolysis conditions of organosolv pulp from kenaf fibers on the physicochemical properties of the obtained nanocellulose, Theor. Exp. Chem. 54 (2018) 193–198, https://doi.org/10.1007/s11237-018-9561-y.
[2] N.P. Klochko, V.A. Barbash, K.S. Klepikova, V.R. Kopach, I.I. Tyukhov, O. V Yashchenko, D.O. Zhadan, S.I. Petrushenko, S. V Dukarov, V.M. Lyubov, A. L. Khrypunova, Use of biomass for a development of nanocellulose-based biodegradable flexible thin film thermoelectric material, Sol. Energy 201 (2020) 21–27, https://doi.org/10.1016/j.solener.2020.02.091.
[3] K. Ushimaru, T. Morita, R. Watanabe, T. Fukuoka, Biobased and mechanically stiff lignosulfonate/cationic-polyelectrolyte/sugar complexes with coexisting ionic and covalent crosslinks, Polym. J. 53 (2021) 1037–1045, https://doi.org/10.1038/s41428-021-00501-2.
[4] H. Seddiqi, E. Oliaei, H. Honarkar, J. Jin, L.C. Geonzon, R.G. Bacabac, J. Klein-Nulend, Cellulose and its derivatives: towards biomedical applications, Cellulose 28 (2021) 1893–1931, https://doi.org/10.1007/s10570-020-03674-w.
[5] Y. Zhi-Long, Y. Ning, Z. Li-Chuan, M. Zhi-Yuan, Z. Yin-Bo, L. Yu-Yang, Q. Bing, X. Wei-Yi, M. Tao, L. Si-Cheng, G. Huai-Ling, W. Heng-An, Y. Shu-Hong, Bioinspired polymeric woods, Sci. Adv. 4 (2022) 7223, https://doi.org/10.1126/sciadv.aat7223.
[6] J. Song, C. Chen, S. Zhu, M. Zhu, J. Dai, U. Ray, Y. Li, Y. Kuang, Y. Li, N. Quispe, Y. Yao, A. Gong, U.H. Leiste, H.A. Bruck, J.Y. Zhu, A. Vellore, H. Li, M.L. Minus, Z. Jia, A. Martini, T. Li, L. Hu, Processing bulk natural wood into a high-performance structural material, Nature 554 (2018) 224–228, https://doi.org/10.1038/nature25476.
[7] D. Sylvain, S. Eduardo, Freezing as a path to build complex composites, Science 311 (2006) 515–518, https://doi.org/10.1126/science.1120937.
[8] U.G.K. Wegst, H. Bai, E. Saiz, A.P. Tomsia, R.O. Ritchie, Bioinspired structural materials, Nat. Mater. 14 (2015) 23–36, https://doi.org/10.1038/nmat4089.
[9] M. E., L.M. E., A.D. H., S. E., T.A. P., R.R. O., Tough, bio-inspired hybrid materials, Science 322 (2008) 1516–1520, https://doi.org/10.1126/science.1164865.
[10] D. Sandberg, A. Kutnar, G. Mantanis, Wood modification technologies - a review, IForest - Biogeosciences For. 10 (2017) 895–908, https://doi.org/10.3832/ifor2380-010.
[11] P. Gerardin, New alternatives for wood preservation based on thermal and chemical modification of wood— a review, Ann. For. Sci. 73 (2016) 559–570, https://doi.org/10.1007/s13595-015-0531-4.
[12] B.G. Compton, J.A. Lewis, 3D-Printing of lightweight cellular composites, Adv. Mater. 26 (2014) 5930–5935, https://doi.org/10.1002/adma.201401804.

[13] Z.-Z. Pan, H. Nishihara, S. Iwamura, T. Sekiguchi, A. Sato, A. Isogai, F. Kang, T. Kyotani, Q.-H. Yang, Cellulose nanofiber as a distinct structure-directing agent for xylem-like microhoneycomb monoliths by unidirectional freeze-drying, ACS Nano 10 (2016) 10689–10697, https://doi.org/10.1021/acsnano.6b05808.
[14] M. Negev, Z. Barnett-Itzhaki, T. Berman, S. Reicher, N. Cohen, R. Ardi, Y. Shammai, T. Zohar, M.L. Diamond, Hazardous chemicals in outdoor and indoor surfaces: artificial turf and laminate flooring, J. Expo. Sci. Environ. Epidemiol. (2021), https://doi.org/10.1038/s41370-021-00396-4.
[15] G. Navaranjan, M.L. Diamond, S.A. Harris, L.M. Jantunen, S. Bernstein, J.A. Scott, T.K. Takaro, R. Dai, D.L. Lefebvre, M.B. Azad, A.B. Becker, P.J. Mandhane, T. J. Moraes, E. Simons, S.E. Turvey, M.R. Sears, P. Subbarao, J.R. Brook, Early life exposure to phthalates and the development of childhood asthma among Canadian children, Environ. Res. 197 (2021), 110981, https://doi.org/10.1016/j.envres.2021.110981.
[16] S. Goulden, M. Negev, S. Reicher, T. Berman, Implications of standards in setting environmental policy, Environ. Sci. Pol. 98 (2019) 39–46, https://doi.org/10.1016/j.envsci.2019.05.002.
[17] M. Chauzar, S. Tateyama, T. Ishikura, K. Matsumoto, D. Kaneko, K. Ebitani, T. Kaneko, Hydrotalcites catalyze the acidolysis polymerization of phenolic acid to create highly heat-resistant bioplastics, Adv. Funct. Mater. 22 (2012) 3438–3444, https://doi.org/10.1002/adfm.201200427.
[18] T. Kaneko, T.H. Thi, D.J. Shi, M. Akashi, Environmentally degradable, high-performance thermoplastics from phenolic phytomonomers, Nat. Mater. 5 (2006) 966–970, https://doi.org/10.1038/nmat1778.
[19] S. Wang, D. Kaneko, K. Kan, X. Jin, T. Kaneko, Syntheses of hyperbranched liquid-crystalline biopolymers with strong adhesion from phenolic phytomonomers, Pure Appl. Chem. 84 (2012) 2559–2568, https://doi.org/10.1351/PAC-CON-12-05-12.
[20] M. Singh, K. Takada, T. Kaneko, Biobased liquid crystalline poly(coumarate)s composites and their potential applications, Compos. Commun. 22 (2020), 100531, https://doi.org/10.1016/j.coco.2020.100531.
[21] M.A. Ali, T. Kaneko, Syntheses of aromatic/heterocyclic derived bioplastics with high thermal/mechanical performance, Ind. Eng. Chem. Res. 58 (2019) 15958–15974, https://doi.org/10.1021/acs.iecr.9b00830.
[22] K. Kan, D. Kaneko, T. Kaneko, Polarized emission of wholly aromatic bio-based copolyesters of a liquid crystalline nature, Polymer 3 (2011), https://doi.org/10.3390/polym3020861.
[23] M. Niaounakis, in: M.B.T.-B.P, P. Niaounakis (Eds.), Chapter 1 - Introduction, William Andrew Publishing, Oxford, 2015, pp. 1–77, https://doi.org/10.1016/B978-0-323-26698-7.00001-5.
[24] A.S. Luyt, S.S. Malik, 16 - can biodegradable plastics solve plastic solid waste accumulation? in: S.M.B.T.-P. to E. Al-Salem (Ed.), Plast. Des. Libr. William Andrew Publishing, 2019, pp. 403–423, https://doi.org/10.1016/B978-0-12-813140-4.00016-9.
[25] A. Oishi, H. Iida, Y. Taguchi, Preparation of poly(butylene succinate) copolymers including L-aspartic acid, Polym. J. 42 (2010) 411–415, https://doi.org/10.1038/pj.2010.16.
[26] Y. Tachibana, M. Yamahata, S. Kimura, K. Kasuya, Synthesis, physical properties, and biodegradability of biobased poly(butylene succinate-co-butylene oxabicyclate), ACS Sustain. Chem. Eng. 6 (2018) 10806–10814, https://doi.org/10.1021/acssuschemeng.8b02112.
[27] S. Shaikh, M. Yaqoob, P. Aggarwal, An overview of biodegradable packaging in food industry, Curr. Res. Food Sci. 4 (2021) 503–520, https://doi.org/10.1016/j.crfs.2021.07.005.
[28] J. Nilsen-Nygaard, E.N. Fernandez, T. Radusin, B.T. Rotabakk, J. Sarfraz, N. Sharmin, M. Sivertsvik, I. Sone, M.K. Pettersen, Current status of biobased and biodegradable food packaging materials: impact on food quality and effect of innovative processing technologies, Compr. Rev. Food Sci. Food Saf. 20 (2021) 1333–1380, https://doi.org/10.1111/1541-4337.12715.
[29] W. Zhang, Y. Xu, P. Wang, J. Hong, J. Liu, J. Ji, P.K. Chu, Copolymer P(BS-co-LA) enhanced compatibility of PBS/PLA composite, J. Polym. Environ. 26 (2018) 3060–3068, https://doi.org/10.1007/s10924-018-1180-0.
[30] O. Platnieks, S. Gaidukovs, A. Barkane, G. Gaidukova, L. Grase, V.K. Thakur, I. Filipova, V. Fridrihsone, M. Skute, M. Laka, Highly loaded cellulose/poly (butylene succinate) sustainable composites for woody-like advanced materials application, Mol 25 (2020), https://doi.org/10.3390/molecules25010121.
[31] S. Nara, T. Komiya, Studies on the relationship between water-satured state and crystallinity by the diffraction method for moistened potato starch, Starch - Stärke 35 (1983) 407–410, https://doi.org/10.1002/star.19830351202.
[32] K.-H. Hsu, C.-W. Chen, L.-Y. Wang, H.-W. Chan, C.-L. He, C.-J. Cho, S.-P. Rwei, C.-C. Kuo, Bio-based thermoplastic poly(butylene succinate-co-propylene succinate) copolyesters: effect of glycerol on thermal and mechanical properties, Soft Matter 15 (2019) 9710–9720, https://doi.org/10.1039/C9SM01958H.
[33] N. Soatthiyanon, C. Aumnate, K. Srikulkit, Rheological, tensile, and thermal properties of poly(butylene succinate) composites filled with two types of cellulose (kenaf cellulose fiber and commercial cellulose), Polym. Compos. 41 (2020) 2777–2791, https://doi.org/10.1002/pc.25575.
[34] R. Chen, W. Zou, H. Zhang, G. Zhang, J. Qu, Crystallization behavior and thermal stability of poly(butylene succinate)/poly(propylene carbonate) blends prepared by novel vane extruder, AIP Conf. Proc. 1713 (2016), 50002, https://doi.org/10.1063/1.4942278.
[35] G.R. A., K. Bhanu, Biodegradable polymers for the environment, Science 297 (2002) 803–807, https://doi.org/10.1126/science.297.5582.803.
[36] A. El-Hadi, R. Schnabel, E. Straube, G. Muller, S. Henning, Correlation between degree of crystallinity, morphology, glass temperature, mechanical properties and biodegradation of poly (3-hydroxyalkanoate) PHAs and their blends, Polym. Test. 21 (2002) 665–674, https://doi.org/10.1016/S0142-9418(01)00142-8.
[37] S. Kamthai, R. Magaraphan, Thermal and mechanical properties of polylactic acid (PLA) and bagasse carboxymethyl cellulose (CMCB) composite by adding isosorbide diesters, AIP Conf. Proc. 1664 (2015), 60006, https://doi.org/10.1063/1.4918424.
[38] I. Debbah, R. Krache, N. Aranburu, A. Etxeberria, E. Perez, R. Benavente, Influence of ABS type and compatibilizer on the thermal and mechanical properties of PC/ABS blends, Int. Polym. Process. 35 (2020) 83–94, https://doi.org/10.3139/217.3858.
[39] S.F. Abdellah Ali, Mechanical and thermal properties of promising polymer composites for food packaging applications, IOP Conf. Ser. Mater. Sci. Eng. 137 (2016), 12035, https://doi.org/10.1088/1757-899x/137/1/012035.
[40] L. Feng, S. Li, S. Feng, Preparation and characterization of silicone rubber with high modulus via tension spring-type crosslinking, RSC Adv. 7 (2017) 13130–13137, https://doi.org/10.1039/C7RA00293A.
[41] B. Sharma, A. Gatoo, M.H. Ramage, Effect of processing methods on the mechanical properties of engineered bamboo, Construct. Build. Mater. 83 (2015) 95–101, https://doi.org/10.1016/j.conbuildmat.2015.02.048.
[42] G.M. Lavers, G.L. Moore, The Strength Properties of Timber, 1969.
[43] D.E. Kretschmann, Effect of Various Proportions of Juvenile Wood on Laminated Veneer Lumber, US Department of Agriculture, Forest Service, Forest Products Laboratory, 1993.
[44] P. Clouston, F. Lam, J.D. Barrett, Incorporating size effects in the Tsai-Wu strength theory for Douglas-fir laminated veneer, Wood Sci. Technol. 32 (1998) 215–226.
[45] S. Kobayashi, H. Uyama, T. Takamoto, Lipase-catalyzed degradation of polyesters in organic solvents. A New methodology of polymer recycling using enzyme as catalyst, Biomacromolecules 1 (2000) 3–5, https://doi.org/10.1021/bm990007c.
[46] Z. Jiang, J. Zhang, Lipase-catalyzed synthesis of aliphatic polyesters via copolymerization of lactide with diesters and diols, Polymer (Guildf) 54 (2013) 6105–6113, https://doi.org/10.1016/j.polymer.2013.09.005.
[47] C.W. Lee, Y. Kimura, J.-D. Chung, Mechanism of enzymatic degradation of poly(butylene succinate), Macromol. Res. 16 (2008) 651–658, https://doi.org/10.1007/BF03218575.
[48] T. Nakajima-Kambe, Y. Shigeno-Akutsu, N. Nomura, F. Onuma, T. Nakahara, Microbial degradation of polyurethane, polyester polyurethanes and polyether polyurethanes, Appl. Microbiol. Biotechnol. 51 (1999) 134–140, https://doi.org/10.1007/s002530051373.
[49] J. Schmidt, R. Wei, T. Oeser, L.A. Dedavid e Silva, D. Breite, A. Schulze, W. Zimmermann, Degradation of polyester polyurethane by bacterial polyester hydrolases, Polymer 9 (2017), https://doi.org/10.3390/polym9020065.
[50] V.M. Pathak, Navneet, Review on the current status of polymer degradation: a microbial approach, Bioresour. Bioprocess. 4 (2017) 15, https://doi.org/10.1186/s40643-017-0145-9.